Bull. Chem. Soc. Jpn., 72, 1887—1898 (1999)

Synthesis and Electronic Properties of d^8 Transition-Metal Complexes of Vinylene-Bridged Bis- and Tris(octaethylporphyrin)s

Hiroyuki Higuchi,* Masatoshi Shinbo, Masanobu Usuki, Makoto Takeuchi, Yutaka Hasegawa, Keita Tani†, and Jūro Ojima

Department of Chemistry, Faculty of Science, Toyama University, 3190 Gofuku, Toyama 930-8555

†Division of Natural Science, Osaka Kyoiku University, 4-698-1 Asahi-oka, Kashiwara, Osaka 582-0026

(Received March 15, 1999)

Complexes of vinylene-bridged bis- and tris(octaethylporphyrin)s (bis(OEP)–M and tris(OEP)–M) with d^8 transition-metal ions (M = Ni(II), Pd(II), and Pt(II)) were synthesized. Metalation of (*E*)-bis(OEP)–H_2 was carried out under the same conditions as for the corresponding octaethylporphyrin complex (OEP–M), to afford a mixture of complexes bearing the vinylene-linkages with (*E*)- and (*Z*)-configurations. On the other hand, metalation of tris(OEP)–H_2 afforded the single product of which two vinylene-linkages remained holding the same (*E, E*)-configuration as that in the free-base. ^{1}H NMR spectra varied more drastically for (*Z*)-bis(OEP)–M, with respect to those of OEP–M, while electronic absorption spectra did more drastically for the (*E*)-isomers. Their electronic properties at the ground state were examined, proving that the interaction between the constituent OEP rings through the vinylene-linkages is more intensive for tris(OEP)–M than for bis(OEP)–M and more intensive for the Ni complex than for the Pd and Pt ones.

In recent years, structurally defined porphyrin-based oligomers bridged with various linkages have been designed for fundamental and applicative studies on the electronic structures and kinetic behaviors to develop new functional organic materials such as opto-electronic devices.[1] Ponomarev et al. reported the synthesis of vinylene-bridged bis(octaethylporphyrin) and its nickel complex (bis(OEP)–M: M = H_2 (**5**) and M = Ni(II) (**6**)),[2] which can be regarded as one of the useful model compounds for the study of "special pair" in the photo-synthetic reaction center.[3] Employing the synthetic methodology for bis(OEP)–M analogously,[2,4] we have successfully synthesized tris(OEP) and its nickel complex (tris(OEP)–M: M = H_2 (**13**) and M = Ni(II) (**14**)) bridged with two vinylene-linkages, and reported that an intensive electronic interaction was observed between three constituent OEP rings, which induced an enhancement of electron-releasing ability and basicity as compared with those of the corresponding mononucleic OEP derivatives (OEP–M: M = H_2 (**1**) and M = Ni(II) (**2**)).[5] In continuation of our investigations on the properties of tris(OEP)–M,[6] synthesis of the Pd and Pt complexes of bis- and tris(OEP)–M were studied, since the electronic structure, i.e., the electronic property of OEP–M is well known to vary intensively with the incorporated metal ions M (Chart 1).[7] Here, we wish to describe the synthesis of d^8 transition-metal ion complexes of the title OEP derivatives starting from (*E*)-bis(OEP)–H_2 (**5**) and (*E, E*)-tris(OEP)–H_2 (**13**) and to discuss their electronic properties as compared with those of the corresponding OEP–M.

Results and Discussion

Synthesis. Synthesis of each series of pairs of (*E*)- and (*Z*)-bis(OEP)–M and of (*E, E*)-tris(OEP)–M was performed

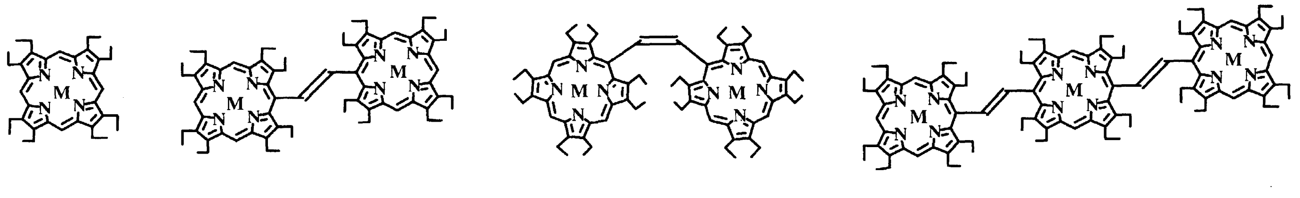

OEP-M

1: M=H_2
2: =Ni
3: =Pd
4: =Pt

(*E*)-bis(OEP)-M

5: M=H_2
6: =Ni
7: =Pd
8: =Pt

(*Z*)-bis(OEP)-M

9: M=H_2
10: =Ni
11: =Pd
12: =Pt

tris(OEP)-M

13: M=H_2
14: =Ni
15: =Pd
16: =Pt

Chart 1.

by metalation of the two free-bases, **5** and **13**, with excessive amounts of the corresponding d^8 transition-metal salts (M(II)X), according to the slightly modified reaction conditions for preparation of OEP–M, as shown in Scheme 1.

It is well known that **5** undergoes isomerization of the vinylene-linkage in refluxed acetic acid (AcOH) to afford an equilibrium mixture of **5** and its (*Z*)-isomer **9** in a ratio of 1 : 2.[8] Although nickelation of OEP–H_2 (**1**) with nickel(II) acetate tetrahydrate ($Ni(OAc)_2 \cdot 4H_2O$) in AcOH is very popular for preparation of OEP–Ni (**2**),[9a] the metalation of **5** to **6** in AcOH was expected to bring complicated results at first. Therefore, **5** was treated with $Ni(OAc)_2 \cdot 4H_2O$ in *N*,*N*-dimethylformamide (DMF) at 110 °C, because it was recently reported that under these conditions the complex **6** was obtained quantitatively from **5** and the (*Z*)-isomer **10** was also obtained in 60% yield along with its mononickelation product (30%) from **9**, respectively.[8a] The reaction of **5** in our case was slightly different from the reported result, but was also successful to afford the corresponding (*E*)-configurational Ni complex **6** in 88% yield together with its (*Z*)-isomer **10** in 7% yield, both of which were fortunately and easily separated by column chromatography on silica gel. Since neither of the already dimetalated compounds **6** and **10** exhibited further isomerization substantially under the same conditions,[10] the above result indicates that the isomerization of (*E*)-vinylene-linkage to (*Z*)-vinylene-linkage in bis(OEP)–H_2 proceeds much faster than the metalation of the free-base OEP. Although clarification for the isomerization processes of the vinylene-linkage should wait for further mechanistic studies, it is curious to mention that nickelation of **5** with $Ni(OAc)_2 \cdot 4H_2O$ in a refluxed mixture of chloroform ($CHCl_3$) and methanol (MeOH), which is also convenient for preparation of **2**,[7a] was not accompanied by such an isomerization, while palladation of **5** in the same medium took place smoothly together with the configurational isomerization (vide infra). Furthermore, it is interesting to note that not only nickelation but also the other metalations of **13** did not exhibit such a configurational isomerization of the vinylene-linkages at all,[6] affording the respective single products with the same configuration as that of **13**, but was accompanied by gradual formation of insoluble materials under the conditions of higher temperatures and longer reaction times.

As mentioned above, by treating **5** with palladium(II) acetate ($Pd(OAc)_2$) in a gently refluxed mixture of $CHCl_3$ and MeOH a pair of (*E*)- and (*Z*)-bis(OEP)–Pd (**7** and **11**) were obtained in 90% and 5% yields, respectively, under much milder conditions than those of the well-known preparative conditions for OEP–Pd (**3**) using palladium(II) chloride ($PdCl_2$) in refluxed benzonitrile (PhCN).[9b] In the case of tris(OEP)–M, incorporation of the Pd(II) ion into **13** also proceeded more readily than that of the Ni(II) ion, being completed within about one-fourth of the reaction time necessary for nickelation of **13**,[5,6] to afford tris(OEP)–Pd (**15**)[11] in an almost quantitative yield.

In the case of platination of **5** and **13**, the reactions were intensively affected by reagent, temperature, and medium. Treatment of **5** with platinum(II) chloride ($PtCl_2$) in refluxed PhCN, which is well known to be convenient for preparation of OEP–Pt (**4**),[9b] gave many insoluble materials along with a very little amount of bis(OEP)–Pt. After several trials, combination of acetylacetonatoplatinum(II) ($[Pt(acac)_2]$)

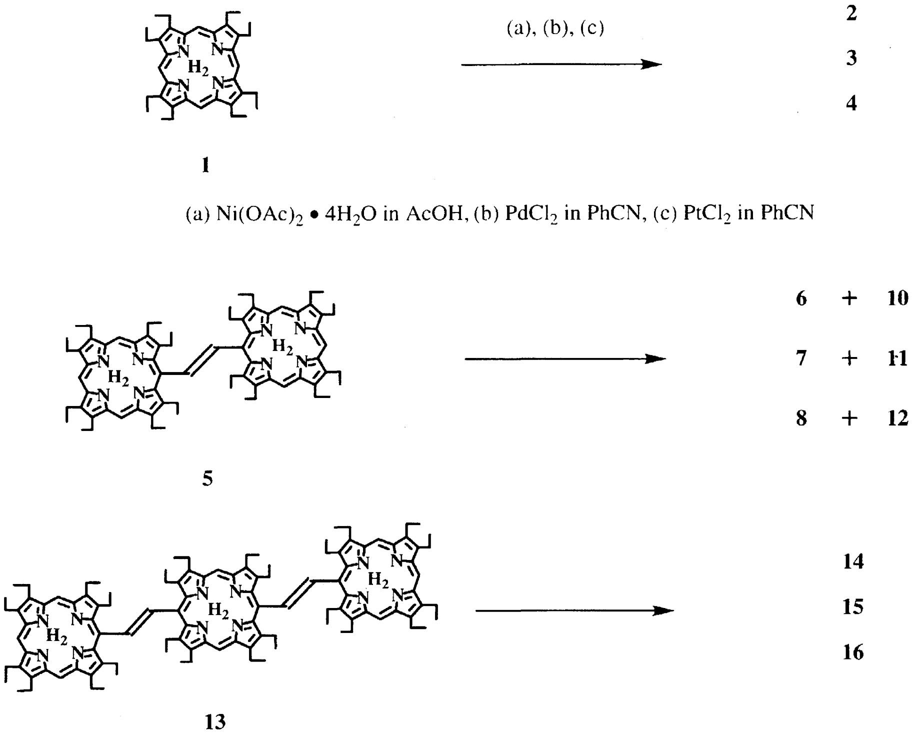

(a) $Ni(OAc)_2 \bullet 4H_2O$ in AcOH, (b) $PdCl_2$ in PhCN, (c) $PtCl_2$ in PhCN

Scheme 1.

with phenol (PhOH)[7] as solvent was found to be quite effective for platination of **5**. Thus, when treated with [Pt(acac)$_2$] in PhOH at 160 °C, a pair of (*E*)- and (*Z*)-bis(OEP)-Pt (**8** and **12**) were obtained in 77% and 11% yields, respectively. On the other hand, it was extremely difficult to incorporate the Pt(II) ion into **13**, as can be deduced from the results in Table 1. In addition to platination with [Pt(acac)$_2$] (in PhOH) or PtCl$_2$ (in CHCl$_3$, PhCN, DMF, or pyridine), treatment of **13** with the easily available platination reagent of *cis*-diamminedichloroplatinum(II) (*c*-[PtCl$_2$(NH$_3$)$_2$]; Cisplatin)[12] (in dioxane, CHCl$_3$–MeOH, H$_2$O–MeOH, PhOH, or DMSO) gave no desired products, mostly affording the starting free-base **13**, otherwise affording insoluble materials without recovery of **13**. This apparently indicates that **13** is thermally less stable than **5**. Then, if one takes into consideration that both nickelation and palladation of **5** and **13** were readily accomplished with the respective reagents of metal(II) acetate, called "acetate method",[7a] platinum(II) acetate (Pt(OAc)$_2$)[13] would be a hopeful reagent. Preliminarily, when the reaction was carried out by using PtCl$_2$ in a refluxed medium of CHCl$_3$ combined with AcOH, a detectable amount for characterization of tris(OEP)–Pt (**16**) was successfully obtained, together with the partially metalated products predicted on the basis of mass spectral measurement. These results imply that Pt(OAc)$_2$ was efficiently formed in a mixture of CHCl$_3$ and AcOH under the equilibrium conditions and that the hardness of acetate anion plays a particularly important role for abstraction of NH protons from each OEP–H$_2$ ring of **5** and **13**. In this respect, [Pt(acac)$_2$] in a refluxed AcOH solution was also found to be useful for platination of **13**. Finally, optimum conditions for platination of **13** were achieved by using 100% AcOH combined with a large excessive amount of PtCl$_2$ or [Pt(acac)$_2$], affording **16** in acceptable yields of 15—30%, though still accompanied by a considerable amount of insoluble material. Nevertheless, when platination of **13** was carried out at the temperature of 70 °C even in a sole solvent of AcOH, which is almost the same as in a refluxed mixture of CHCl$_3$ and AcOH (5 : 2), the yield of **16** was drastically reduced. Although the reason for these results is not clear at present, it is obvious that both acetate ion and reaction temperature exert influences on the platination of **13**.

^{1}H NMR Spectra. ^{1}H NMR spectra of all bis- and tris(OEP)–M as well as OEP–M were measured at room temperature, unless otherwise stated. Chemical shifts of the selected meso and vinylene protons, as named in the respective structures of the OEP derivatives (Chart 2), are summarized in Table 2.

(I) Comparison of (*E*)-Bis(OEP)–M and Tris(OEP)–M with OEP–M: The chemical shift of the *meso* proton Ha of OEP–M can be regarded as a measure for the magnitude of diamagnetic ring current effect induced in a diaza[18]annulene ring system.[14] As can be seen in a series of OEP–M (**1**—**4**), Ha shifts to the up-field in the order of M = H$_2$ ≈ Pd → Pt → Ni, clearly indicating the smallest ring current for the Ni complex **2**. Hb and Hc of bis(OEP)–M (**5**—**8**) varied almost in parallel with Ha of OEP–M and both protons possessed the similar chemical shifts, though the latter ones largely exhibited a slightly greater up-field shift from the corresponding ones. The similar trend of chemical shift changes with the incorporated metals was also observed for all the *meso* protons Hd, He, and Hf of tris(OEP)–M (**13**—**15**), suggesting that each OEP ring of this type of oligomers connected with the vinylene-linkage retains and reflects the inherent ring current of OEP–M.

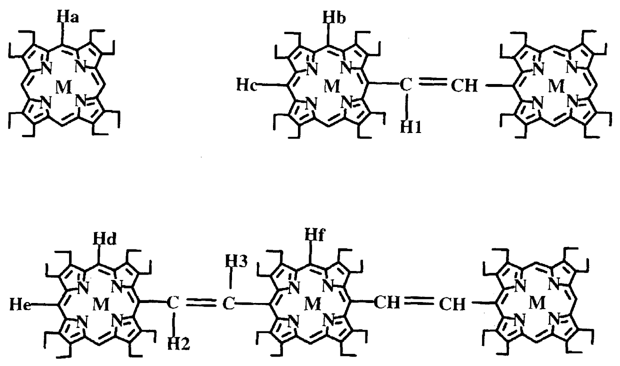

Chart 2.

Table 1. Platination of **13** with 20 Molar Amounts of Pt(II)X under Various Conditions to **16**

Pt(II)X	[reaction media, temperature, and time, results]
PtCl$_2$	[CHCl$_3$, reflux, 10 h, no reaction] [PhCN, DMF, or pyridine, reflux, ca. 8 h, none[a)]] [CHCl$_3$–AcOH (5 : 2), refulx 55 h, 4% and others[b)]] [AcOH, 70 °C, 44 h, 2% and others[b)]] [AcOH, reflux, 6 h, 20—, 28%]
c-[PtCl$_2$(NH$_3$)$_2$]	[1,4-dioxane, CHCl$_3$–MeOH, or H$_2$O–MeOH, refulx, ca. 10 h, no reaction] [PhOH, DMF, or DMSO, reflux, ca. 5 h, none[a)]]
[Pt(acac)$_2$]	[PhOH, 180 °C, 3 h, none[a)]] [AcOH, reflux, 5 h, 15—25%]

a) Insoluble materials without recovery of **13**. b) Contains a small amount of mono- and dimetalated products together with insoluble materials.

Table 2. Chemical Shifts (/ppm) of *meso* (Alphabetical) and Vinylene (Numerical) Protons for OEP–M, Bis(OEP)–M, and Tris(OEP)–M

M	Ha (4H)	Hb (4H)	Hc (2H)	H1 (2H)	Hb (4H)	Hc (2H)	H1 (2H)	Hd (4H)	He (2H)	Hf (2H)	H2 (2H)	H3 (2H)
	OEP–M	(*E*)-Bis(OEP)–M			(*Z*)-Bis(OEP)–M			Tris(OEP)–M				
H_2	10.10	10.13	9.94	8.57	8.03	9.50	9.69	10.07	9.89	9.68	8.57	8.48
Ni	9.76	9.48	9.50	7.67	8.06	9.05	9.29	9.44	9.49	9.30	7.64	7.53
Pd	10.12	10.08	10.04	8.18	8.15	9.26	9.55	10.08	10.04	9.99	8.16	8.03
Pt	10.02	10.02	9.96	8.17	8.11	9.21	9.42	10.00	9.97	9.93	8.18	8.02

To look at the chemical shift changes for meso protons more cautiously, it is also proved that the extent of reduction of the ring current effect of OEP–M depends on both the degree of oligomerization and the kind of incorporated metals. In the case of series of the free-bases and Ni complexes, meso protons showed the up-field shift in the order of OEP–M → bis(OEP)–M → tris(OEP)–M, may be ascribed to the reduction of the respective OEP ring currents in the same order. Furthermore, Hd and He protons attached to the outer OEP rings of tris(OEP)–M exhibited only a little up-field shift from the corresponding meso protons of OEP–M and bis(OEP)–M, while Hf proton attached to the central OEP ring appeared at the greater up-field position than Hd and He. The reason for such an up-field shift of Hf (δ = 9.30) from Hd and He (δ = 9.44 and 9.49) in tris(OEP)–Ni (**14**), for example, can be attributed to the steric hindrance between the peripheral ethyl groups and two vinylene-linkages as substituent at 5 and 15 positions of the central OEP ring rather than to the inductive effect of the vinylene-linkage,[15] causing the severe distortion of the central OEP ring plane and thus resulting in the more reduction of the central OEP ring current. This is supported by some evidence of the much broader signals due to Hf protons at around room temperature, which arises from an atrope isomerism between U,U- (or D,D-) and U,D-conformers in consequence of distortion of the central OEP ring in tris(OEP)–M,[5,6,15] affecting not only the line shape but also the chemical shift (Fig. 1).

The behavior of both Pd and Pt complexes, however, seems to be different from that of the free-bases and Ni complexes. For example, tris(OEP)–Pd (**15**) as well as bis(OEP)–Pd (**7**) possessed almost the same chemical shifts for all *meso* protons, with the inherent ring current of OEP–Pd (**3**) remaining unchanged to a great extent. These facts indicate that connection with the vinylene-linkage does not perturb the OEP frameworks of the Pd and Pt complexes, i.e., the respective ring currents of OEP–M in **3** and **4**, so intensively as those in **1** and **2**.

Chemical shift changes for vinylene protons with the incorporated metals were different from those for *meso* protons, resulting in up-field shifts in the order of M = $H_2 \rightarrow Pd \approx Pt \rightarrow Ni$ in all series. Also, it is worthy of note that the vinylene protons in tris(OEP)–M possessed almost the same chemical shifts as those in bis(OEP)–M, as can be seen in the trend observed for the meso protons, though H3 near by the central OEP ring appeared at the slightly higher field than H2. These results indicate that tris(OEP)–M is a system simply extended from the corresponding bis(OEP)–M, with high similarities in the structural properties.

Based on the results observed above, it is supposed that, in the case of the free-bases and Ni complexes, the vinylene-linkages in solution are situated within a deshielding region of diamagnetic ring current effect from the OEP rings and thus take part in the full π-electronic conjugation system through the whole molecule to a considerable extent. On the other hand, in the case of the Pd and Pt complexes, the vinylene-linkages are outside such a deshielding region and thus impede the π-electronic conjugation between the OEP rings through the vinylene-linkage more or less, as illustrated in Fig. 1. In other words, the activation energies for interconversion between U,U- (or D,D-) and U,D-conformers

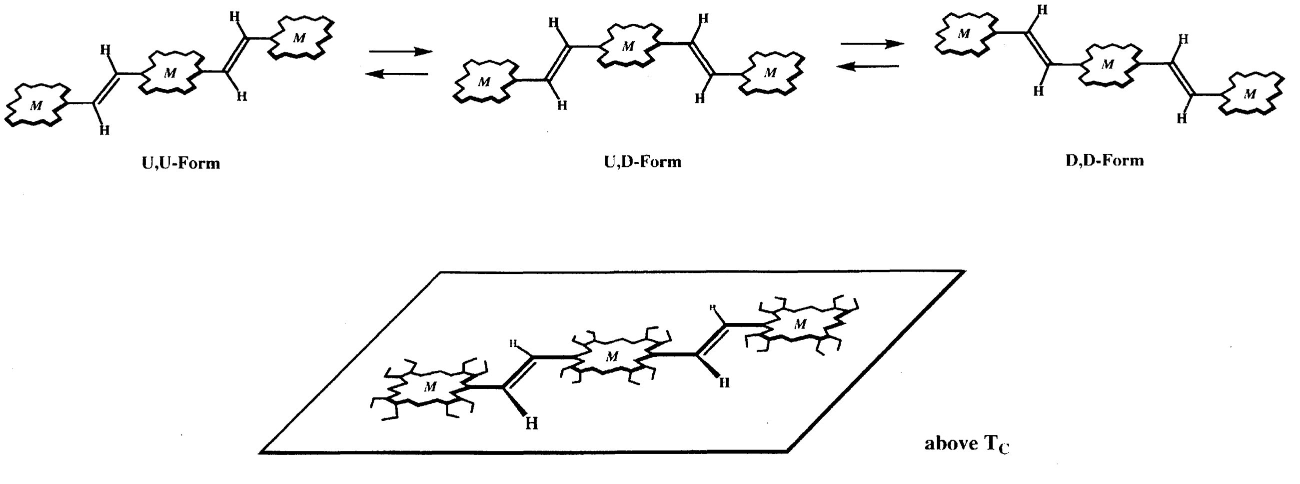

Fig. 1. Interconversion between U,U (D,D)-Form and U,D-Form for tris(OEP)-M.

in tris(OEP)–Pd and –Pt complexes would be much greater than those in the free-base and Ni complex. Attempts to determine their coalescence temperatures (T_c) by means of ^{1}H NMR spectroscopy were unsuccessful, since either of the most soluble Ni complexes of bis- and tris(OEP)–M was deposited out of chloroform solution at the lower temperature.[6] In relation with this speculative conclusion, it is worthy of note that (*E*)-bis(OEP)–Ni (**6**) was studied by means of X-ray crystallography by Kitagawa et al. and was proved to exist in a stairway-like conformational structure around the vinylene-linkage where two constituent saddle-shaped OEP rings are situated in an almost parallel orientation.[16] Consequently, it is likely that such a stairway structure makes the Pd and Pt complexes of bis- and tris(OEP)–M retain the inherent ring current effects of the Pd and Pt complexes of the mononucleic OEP–M and thus shift their vinylene protons to a more up-field position than the free-base and Ni complex. Even though the vinylene protons of the Ni complexes are within a deshielding region, the reason why their vinylene protons resonate at such higher fields should be ascribed to the smaller ring current of the OEP–Ni complex itself[14] (also see Electronic Spectra).

(II) Comparison of (*Z*)-Bis(OEP)–M with (*E*)-Bis(OEP)–M: Peripheral ethyl substituents in (*Z*)-bis(OEP)–M were intensively affected by configurational change: the methylene protons appeared at higher fields and over a wider range, as compared with those in (*E*)-isomer.[8] Both *meso* and vinylene protons in (*Z*)-bis(OEP)–M also exhibited distinct behaviors from the corresponding protons in (*E*)-isomer. The signals due to meso protons Hb and Hc appeared in reverse between (*E*)- and (*Z*)-bis(OEP)–M, both Hb and Hc in (*Z*)-bis(OEP)–M exhibited up-field shift from the corresponding protons in (*E*)-isomer, and especially chemical shift of Hb was given at a field higher by 1.7—2.1 ppm than that of Ha in OEP–M. Table 2 also shows that respective chemical shifts of Hb in (*Z*)-isomer did not change in the same direction as those of Hc as against M; up-field shifts for Hb were in the order of M = Pd → Pt → Ni → H_2 over a range of 0.12 ppm and for Hc in the order of M = H_2 → Pd → Pt → Ni over a range of 0.45 ppm. In opposition to the behavior of *meso* protons, the vinylene proton H1 in (*Z*)-bis(OEP)–M exhibited down-field shift from that in (*E*)-isomer, appearing at the lower field than *meso* protons, apart from Hc by 0.2—0.3 ppm and from Hb by 1.2—1.7 ppm, and curiously changed its chemical shift in the same direction as the *meso* proton Hc according to M. And yet, the magnitude of up-field shift of Hb from Ha is much smaller for the Ni complex **10** (Hb–Ha: $\Delta\delta = 1.70$) and the magnitude of down-field shift of H1 from (*E*)-bis(OEP)–M to (*Z*)-isomer is oppositely much greater for **10** ($\mathrm{H1}_{(Z)-(E)}$: $\Delta\delta = 1.62$), as compared with the magnitudes of the corresponding chemical shift changes for the other complexes **9**, **11**, and **12** (Hb-a: $\Delta\delta = 1.93$—2.07 and $\mathrm{H1}_{(Z)-(E)}$: $\Delta\delta = 1.12$—1.37).

These results indicate that two OEP-M rings in (*Z*)-bis(OEP)–M face to each other with some dihedral angle θ depending on M, as depicted in Fig. 2. In other words, through the configurational change from (*E*)-bis(OEP)–M to (*Z*)-isomer, Hb and Hc moved into the more shielding region, while H1 moved into the more deshielding region. As can be deduced from Fig. 2, the larger (smaller) dihedral angle (θ) would make the distance between the face-to-face stacked meso protons longer (shorter) and oppositely the distance between the neighboring vinylene protons shorter (longer), resulting in a decrease (an increase) of anisotropic ring current effect to Hb and in an increase (a decrease) of steric compression to H1. As discussed in Section I, each OEP ring of this type of oligomer connected with the vinylene-linkage substantially retains and reflects the inherent ring current of OEP–M more or less. In this respect, if the dihedral angles θ are the same for all (*Z*)-bis(OEP)–M, the smaller up-field shift of Hb for the Ni complex **10**, which is more sensitive to the anisotropic effect in (*Z*)-bis(OEP)–M than another *meso*-proton Hc as aforementioned, could be interpreted simply by regarding its smallest ring current. However, the greater down-field shift of H1 for **10** seems hard to be explained only by the small ring current. These chemical shift changes of Hb-a and $\mathrm{H1}_{(Z)-(E)}$, suggesting a structural difference of the Ni complex **10** from the other metal complexes, would lead to a conclusion of the larger θ for **10**.

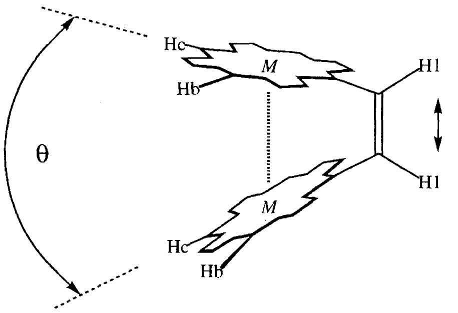

Fig. 2. Transannular interaction between the face-to-face stacking OEP–M rings in (*Z*)-bis(OEP)–M.

If one takes the conversion of (*E*)-bis(OEP)–H_2 to the sterically more crowded (*Z*)-isomer at the higher temperatures into consideration,[8,10] some preference in an attractive interaction between two OEP–M rings should be supposed for (*Z*)-isomer. From ^{1}H NMR studies on (*Z*)-bis(OEP)–M, it is also predicted that the nature of incorporated metals influences the degree of dihedral angle θ reflecting such an interaction between two faced OEP–M rings, which is expected to be less intensive for the Ni complex **10**. Although it is premature to make a conclusive discussion on the nature of interaction at this stage, these results indicate that such a transannular interaction plays an important role to give rise to the peculiar chemical and electronic properties of (*Z*)-bis(OEP)–M[3,4,8,10] (see Sections IV and VI).

Electronic Absorption Spectra. Electronic absorption spectra of bis- and tris(OEP)–M as well as OEP–M were measured in $CHCl_3$ and absorption spectral data of their Soret and Q bands are summarized in Table 3.

(III) Comparison of (*E*)-Bis(OEP)–M and Tris(OEP)–M with OEP-M: It is well known that d^8 transition-metal ion complexes of OEP-M belong to a class of hypso type, in which both Soret and Q bands of **2**—**4** shift to the

Table 3. Absorption Spectral Data (λ_{max}/nm, (log ε)) for OEP–M, Bis(OEP)–M, and Tris(OEP)–M in $CHCl_3$

M	Soret bands and Q bands							
	OEP–M		(*E*)-Bis(OEP)–M		(*Z*)-Bis(OEP)–M		Tris(OEP)–M	
H_2	375 sh (4.96) 399 (5.25)	498 (4.13) 536 (3.97) 567 (3.37) 618 (3.63)	380 sh (5.05) 421 (5.37)	480 sh (4.55) 510 (4.52) 546 (4.17) 581 (4.18) 634 (3.86) WAB	330 sh (4.62) 390 (5.25)	474 sh (4.42) 528 (4.18) 594 (3.86) 651 (3.43) VWAB	375 sh (5.06) 414 (5.43) 430 sh (5.32)	507 (4.83) 541 sh (4.58) 580 (4.40) 633 (4.26) WAB
Ni	330 (4.10) 370 sh (4.44) 393 (5.37)	516 (4.06) 552 (4.57)	405 sh (5.19) 417 (5.37)	483 (4.51) 535 (4.29) 568 (4.36) WAB	392 (5.29)	530 (4.32) 564 (4.45) VWAB	408 (5.42) 421 sh (5.33)	491 sh (4.78) 516 sh (4.73) 564 (4.64) WAB
Pd	325 (3.95) 393 (5.38)	515 (4.10) 546 (4.77)	400 sh (5.17) 417 (5.35)	525 (4.32) 556 (4.49)	330 sh (4.43) 391 (5.29)	534 (4.11) 567 (4.20)	409 (5.44) 427 (5.37)	530 (4.48) 554 (4.61) 561 (4.58)
Pt	327 (3.80) 357 sh (4.10) 381 (5.41)	505 (3.94) 538 (4.70)	388 sh (5.22) 402 (5.38)	515 (4.30) 545 (4.63)	380 (5.37) 405 sh (5.04)	522 (4.32) 549 (4.50)	393 (5.48) 411 (5.32)	519 (4.41) 544 (4.69) 549 sh (4.68) 565 sh (4.25)

WAB: weak absorption bands tailing up to 900—1100 nm. VWAB: very weak absorption bands tailing up to 650—750 nm.

shorter wavelengths from those of OEP–H_2 (**1**),[7] with absorption bands becoming much sharper and simpler in consequence of the higher electronical symmetry (D_{4h}) caused by metalation of the D_{2h} symmetric free-base **1**. With respect to Q bands, four maxima of 498, 536, 567, and 618 nm for **1** degenerate into two maxima within a region between 500 and 555 nm for **2**—**4**. On the other hand, the Soret bands of OEP–M exhibit hypsochromic shift in order of M = H_2 (**1**) → Ni (**2**) ≈ Pd (**3**) → Pt (**4**), over a range of ca. 20 nm, proving quite evident with the Pt complex **4**. Almost the same trend of hypsochromic shift of the Soret bands as for OEP–M was observed for bis(OEP)—M; M = H_2 (**5**) → Ni (**6**) ≈ Pd (**7**) → Pt (**8**), with their absorption bands appearing at the longer wavelengths than the corresponding bands for OEP–M. The same trend of hypsochromic shift of Soret bands was also observed for tris(OEP)–M, but their main bands appeared at the wavelengths between those of the corresponding OEP–M and bis(OEP)–M.

Apart from such a high similarity in hypsochromic shift of both Soret and Q bands between these three series of the OEP–M derivatives, some differences between them were observed in weak absorption bands (WAB) with long tails, which are believed to be characteristic of the electronic interactions between the constituent OEP rings in bis- and tris(OEP)–M.[2,5,6] In the case of OEP–M, none of **1**—**4** exhibit any absorption bands in the region of wavelengths longer than 620 nm. On the other hand, the Ni complexes of both bis- and tris(OEP)–M (**6** and **14**) possessed the distinct absorptions reaching up to 1000 nm similarly to the corresponding free-bases (**5** and **13**), indicating the existence of electronic interaction between the constituent OEP rings through the vinylene-linkages at the ground state, as shown in Fig. 3(a). The Pd complexes (**7** and **15**) as well as the Pt complexes (**8** and **16**), however, did not show such absorptions in a region of wavelengths longer than 600 nm at all, affording the very simple Q bands with two main vibrations and with enhanced intensities, quite similar to those for the mononucleic OEP–Pd and –Pt complexes (Fig. 3(b) for **3** and **4**).

As discussed in the case of OEP–M,[7] these spectral behaviors of bis- and tris(OEP)–M might also reflect the magnitude of back-bonding interaction between M and OEP. The back-donation from M to OEP, which is more pronounced with the

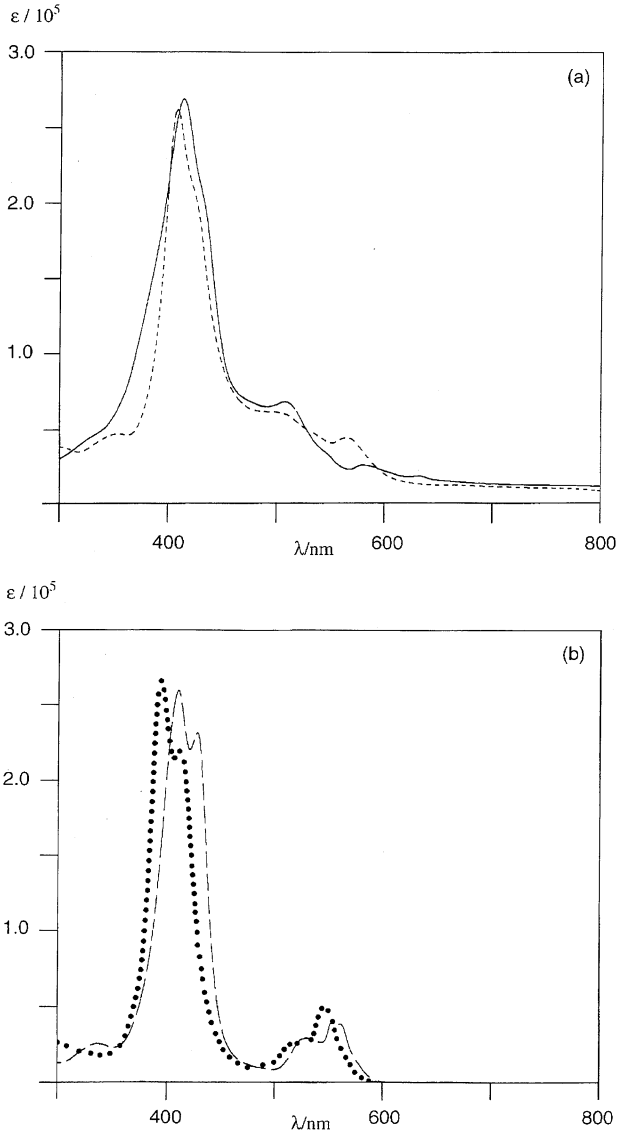

Fig. 3. Electronic absorption spectra of tris(OEP)–M; (a) for **13** (——) and **14** (- - -) and (b) for **15** (– – –) and **16** (····) in $CHCl_3$.

heavier metals, operates to push LUMO levels of OEP up and HOMO level down, resulting in the larger HOMO-LUMO gaps. In the case of the free-bases (**5** and **13**) and Ni complexes (**6** and **14**), the constituent OEP rings interact mutually through the vinylene-linkage to achieve the full π-electronic conjugation for stabilization, since the back-bonding interaction between Ni and OEP ring does not produce stabilization energy so sufficiently as the full π-electronic conjugation. In contradistinction to the stabilization from the π-electronic conjugation, it is also evident that such π-electronic conjugation in the molecule of this type, which forces the whole molecule to exist in a planar conformational structure more or less, involves a disadvantage of steric repulsion between the peripheral ethyl substituents and the vinylene-linkages. In this respect, the back-bonding interaction in the Pd (**7** and **15**) and Pt complexes (**8** and **16**) is sufficient to compensate such an uncomfortable stabilization from the π-electronic conjugation. This results in a strong tendency that the respective OEP ring chromophores in the Pd and Pt complexes exist independently. In other words, the stronger back-bonding interaction between M and OEP causes deformation from the full π-electronic conjugation planar conformation around the vinylene-linkage into a stairway structure to a greater extent, as is also speculated from ^{1}H NMR spectral behaviors of bis- and tris(OEP)–M (Fig. 4). Nevertheless, the fact that both pairs of **7** and **8** and of **15** and **16** exhibited their Soret bands at the wavelengths longer by over 20 nm than the mononucleic OEP–M pair of **3** and **4** also suggests the existence of through-space interaction between the constituent OEP rings.

(IV) Comparison of (*Z*)-Bis(OEP)–M with (*E*)-Bis(OEP)–M: As an example of a pair of (*E*)- and (*Z*)-bis(OEP)–M, absorption spectra of the Pt complexes **8** and **12** are shown in Fig. 5. The Soret band for (*Z*)-bis(OEP)–Pt (**12**) appeared at the wavelength shorter by ca. 20 nm than that for the (*E*)-isomer **8**, resulting in giving almost the same maximum as for OEP–Pt (**4**). This is nearly the same tendency for the other pairs of bis(OEP)–M complexes. The way the behavior of hypsochromic shift of the Soret bands varied with the incorporated metal M in (*Z*)-bis(OEP)–M was very similar to that in a series of (*E*)-isomers, resulting in a quite eminent shift for the Pt complex. As can also be seen in Fig. 5, both Soret and Q bands for (*Z*)-isomer are fairly broad as compared with those for (*E*)-isomer.

Such behaviors are characteristic of the electronic absorption spectra for (*Z*)-bis(OEP)–M. Even the free-base and Ni complex, whose structural properties are distinct from those of the Pd and Pt complexes among a series of (*E*)-bis(OEP)–M, exhibited similar behavior to the above. Such a high similarity in spectral behavior of the Soret bands between (*Z*)-bis(OEP)–M and the mononucleic OEP–M indicates not only an electronical isolation of the respective OEP rings in the dinucleic (*Z*)-isomer but also a small substituent

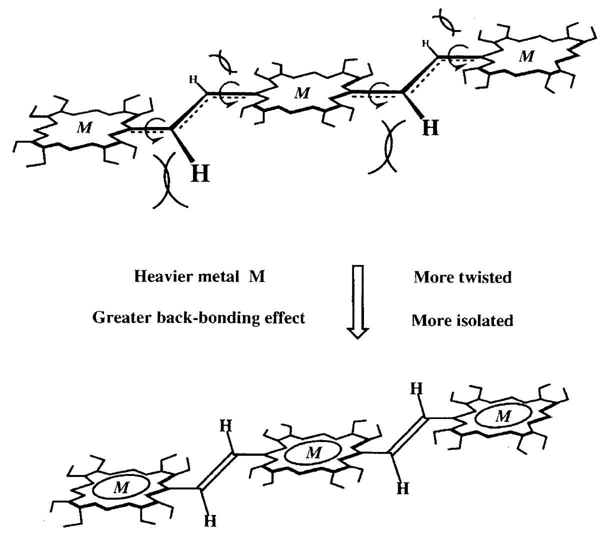

Fig. 4. Conformational changes of tris(OEP)–M from the π-electronic conjugation plane to the more stairway-like structure by metalation with the heavier metal M.

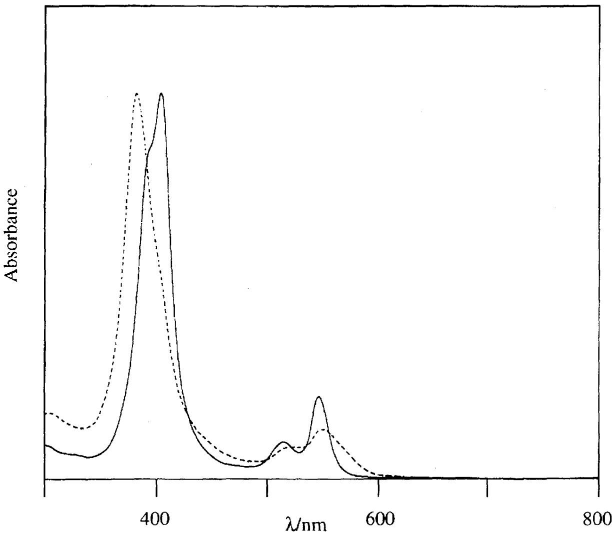

Fig. 5. Electronic absorption spectra of (*E*)-bis(OEP)–Pt (**8**: —) and (*Z*)-bis(OEP)–Pt (**12**: - - -) in $CHCl_3$.

effect of the vinylene-linkage on the electronic property of OEP–M. On the contrary, such a broadening of the whole spectra for (*Z*)-isomer suggests a transannular interaction between two faced OEP–M rings, as deduced from the structure illustrated in Fig. 2, though it can not be excluded yet from a probable reason if the face-to-face stacking structure induces an elongation of equilibrium nuclear distances at the excited state in this system. It remains to be proved how such a transannular interaction, which arises most likely from the exciton coupling between two faced OEP–M rings,[16] affects the back-bonding interaction of the incorporated metals M with OEP.

Cyclic Voltammetry. Electrochemical properties of bis- and tris(OEP)–M as well as those of OEP–M were examined by means of cyclic voltammetry. Voltammograms for the Ni complexes (**2**, **6**, **10**, and **14**), for example, are given in Fig. 6. Initial direction of scanning was anodic (oxidation) for all compounds and the respective voltammograms at the first scan between 0 and +1.8 V were taken for discussion, especially because a configurational isomerization of the vinylene-linkage potentially takes place in all compounds of bis- and tris(OEP)–M.[17] Their electron-releasing abilities were estimated from the first oxidation potential E_1 values (Table 4).

(V) Comparison of (*E*)-Bis(OEP)–M and Tris(OEP)–M with OEP–M: Oxidation of a series of OEP–M including the free-base **1** proceeds via two one-electron transfer processes to afford the corresponding dications. Radical cations, the products at the first oxidation stage, form at the respective potentials regularly in accordance with ionization tendency of M, indicating the highest electron-releasing abil-

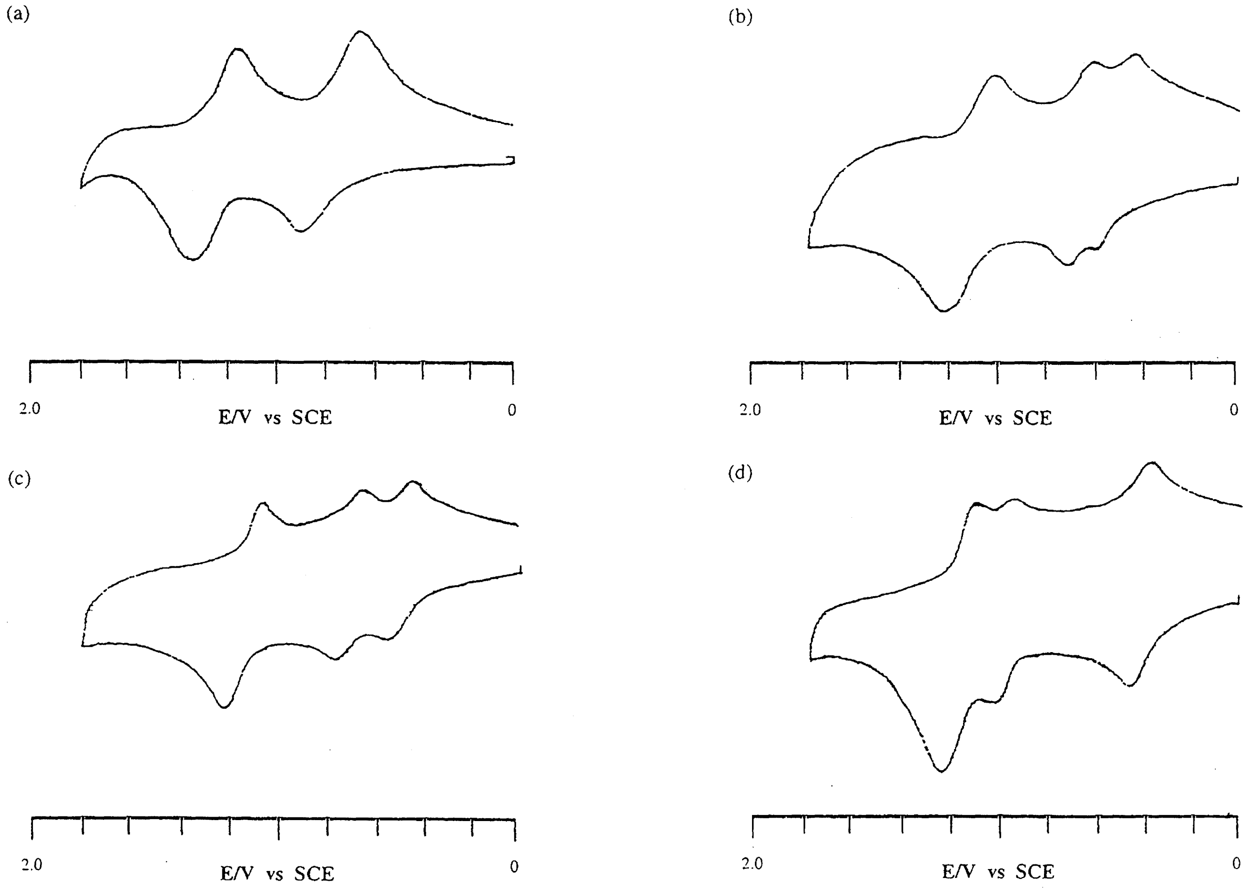

Fig. 6. Voltammograms of (a) OEP–Ni (**2**), (b) (*E*)-bis(OEP)–Ni, (**6**), (c) (*Z*)-bis(OEP)–Ni (**10**), and (d) tris(OEP)–Ni (**14**).

Table 4. Half-Wave Oxidation Potentials for OEP–M, Bis(OEP)–M, and Tris(OEP)–M

M	OEP–M		(*E*)-Bis(OEP)–M			(*Z*)-Bis(OEP)–M			Tris(OEP)–M		
	$E_1^{1/2}$(1e)	$E_2^{1/2}$(1e)	$E_1^{1/2}$(1e)	$E_2^{1/2}$(1e)	$E_3^{1/2}$(2e)				$E_1^{1/2}$(2e)	$E_2^{1/2}$(1e)	$E_3^{1/2}$(3e)
H_2	0.94	1.44	0.59	0.72	1.49	0.56	0.67	1.42	0.36	0.56	1.19
Ni	0.86	1.32	0.62	0.70	1.23	0.57	0.76	1.26	0.49	1.05	1.25
Pd	1.04	1.78	0.72	0.90	1.41	0.61	0.94	1.47	0.65	1.14	1.48
Pt	1.09	1.81	0.86	1.04	1.52	0.61	0.98	1.47	0.75	1.17	1.56

Oxidation potentials (E_{ox}/V) were measured by cyclic voltammetry in CH_2Cl_2 containing *n*-Bu_4NClO_4. GC (working *E*), Pt (counter *E*), and SCE (reference *E*). Scan rate; 120 mV s^{-1}.

ity of the Ni complex **2**.[18] On the other hand, both bis- and tris(OEP)–M exhibited three redox waves reversibly. Similarly, the final products were tentatively assigned to be the corresponding bis- and tris(dication)s (vide infra).[19] The first oxidation potential E_1 values of both bis- and tris(OEP)–M, however, became higher for the complex with the heavier metal, resulting in the highest electron-releasing ability for the free-base in each series, which seemingly correlates with the behavior of hypsochromic shift of their Soret bands in the electronic spectra. In other words, the heavier effect, i.e., the greater back-bonding interaction between OEP and M makes the respective OEP–M more isolated to lower their HOMO levels and thus makes the radical-cationic site less delocalized throughout the whole molecule for stabilization, decreasing the electron-releasing abilities of tris(OEP)–M in order of M = H_2→Ni→Pd→Pt. Also, it is proved that oligomerization of OEP–M with the vinylene-linkage lowers its E_1 value in order of the number of OEP ring, resulting in the highest electron-releasing ability for tris(OEP)–M in each series of the complexes with the same metal. Since the substituent effect of the vinylene-linkage on the electrochemical property of OEP–M is very small,[17b] this result suggests an existence of through-space interaction between the respective OEP–M rings to elevate their HOMO levels regularly. Thus, the change in E_1 values from M = H_2 up to M = Pt of tris(OEP)–M is comparable to that from OEP–Ni (**2**) up to tris(OEP)–Ni (**14**), in spite of the reversed influences. This is the same case for the Pd complexes.

Although both bis- and tris(OEP)–M exhibited three oxidation waves, the number of electrons participating in each redox step proved to be different between them by current ratio analyses; for bis(dication)s via one-, one-, and two-electron transfer processes and for tris(dication)s via two-, one-, and three-electron transfer processes. Products at the re-

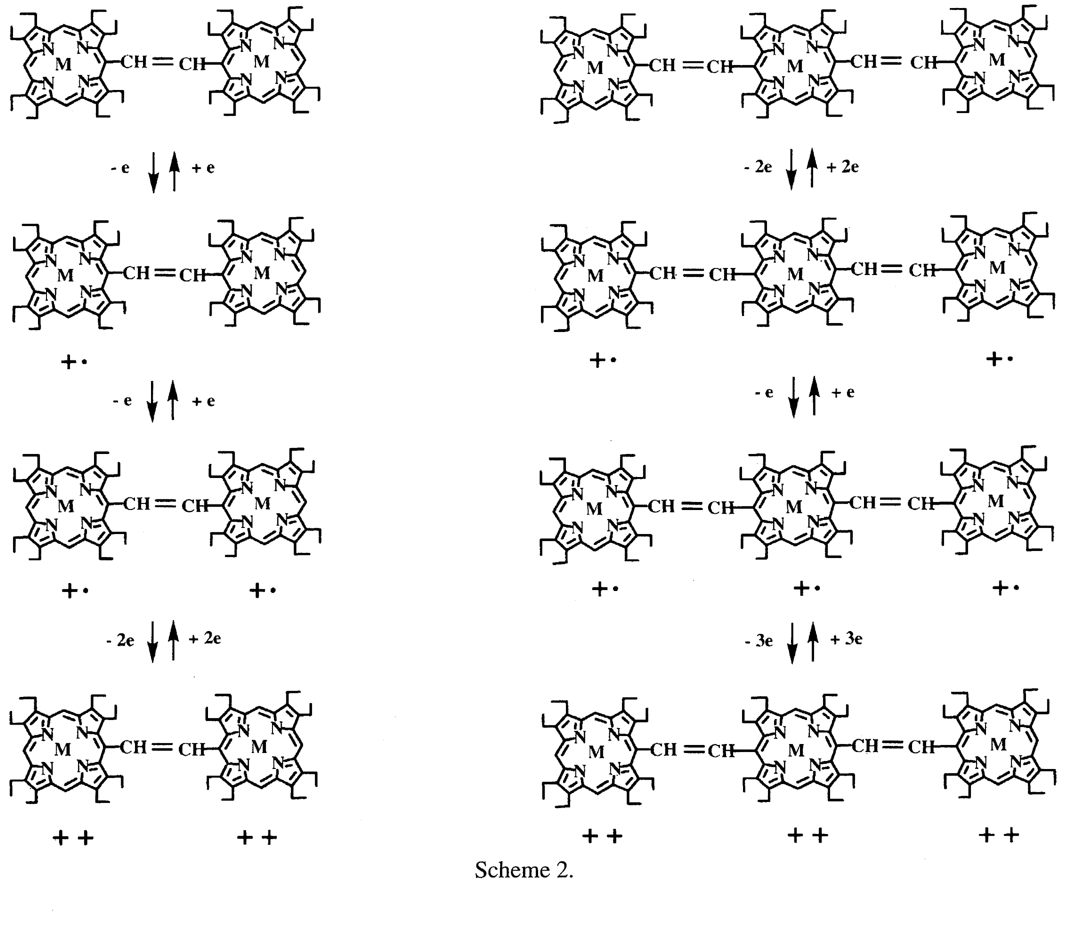

Scheme 2.

spective steps were proposed mechanistically based on these results, as shown in Scheme 2. Particularly in the case of tris(OEP)–M, the species of bis(radical cation) formed at the first stage was tentatively deduced from the fact that the basicity of the outer OEP–H_2 in **13** is much higher than that of the central OEP–H_2.[5] As compared with a small difference between E_1 and E_2 values for bis(OEP)–M, tris(OEP)–M exhibited a fairly large difference between E_1 and E_2 values, indicating a disadvantage in activation energy for releasing the next one electron from the bis(radical cation) which newly introduces the radical-cationic site into the central OEP–M ring sandwiched between two radical-cationic OEP–M ones.

(VI) Comparison of (*Z*)-Bis(OEP)–M with (*E*)-Bis(OEP)–M: As can be seen in Table 4, the second oxidation E_2 values for (*Z*)-bis(OEP)–M are different between groups of the free-base and Ni complex (**9** and **10**) and of the Pd and Pt complexes (**11** and **12**) similarly to the corresponding (*E*) isomers, while their E_1 values are almost unchanged as against M. Table 4 also shows that (*Z*)-bis(OEP)–M exhibits lower oxidation potential E_1 values than the corresponding (*E*)-isomers, proving that the electron-releasing abilities of (*Z*)-bis(OEP)–M were enhanced more than those of the (*E*)-isomers. Moreover, among a series of the Pd complexes (**3**, **7**, **11**, and **15**), **11** exhibited the lowest oxidation potential E_1 value, resulting in a greater electron-releasing ability of the dinucleic complex as compared with the trinucleic one. The same trend was found to be more pronounced with a series of the Pt complexes (**4**, **8**, **12**, and **16**).

These results indicate that the transannular interaction between two faced OEP rings in the neutral state of (*Z*)-bis(OEP)–M is intensive sufficiently to suppress not only the back-bonding interaction between the OEP ring and M but also the through-space interaction between the constituent OEP rings in (*E*)-bis- and tris(OEP)–M. Such an intensive transannular interaction is likely to cause the fact that (*E*)-bis(OEP)–H_2 is converted preferably to the sterically more crowded (*Z*)-isomer at the higher temperatures.[8,10] Especially, the magnitude of the transannular interaction can be expected to be outstanding for (*Z*)-bis(OEP)–Pt (**12**), leading to the much smaller dihedral angle θ (Fig. 2) than that for the free-base (**9**) and that for the Ni complex (**10**), as is consistent with the results from ^{1}H NMR spectra (see Section II). Furthermore, from the fact that the E_2 values for (*Z*)-bis(OEP)–M were dependent on M almost in parallel with those for the (*E*)-isomers, it is indicated that the back-bonding interaction also plays an important part in stabilizing the first oxidation products, radical cations, from (*Z*)-isomers.

Conclusion

Tris(OEP)–M was found to possess a system simply extended from the corresponding (*E*)-bis(OEP)–M, with the high similarities in conformational properties. It is also proved that metalation of the bis- and tris(OEP) free-bases, **5** and **13**, with d^8 transition-metal ions induces deformation from the π-electronic conjugation planarity throughout the whole molecule to the stairway-like conformational structure, in accordance with the magnitudes of back-bonding interaction between OEP and the incorporated metals M (M = $H_2 \rightarrow Ni \rightarrow Pd \rightarrow Pt$), as illustrated in Fig. 4. This brings on the reduction of the through-bond interaction between the constituent OEP rings in the same order, resulting in the largest degree of hypsochromic shift and in the lowest electron-releasing ability for the Pt complexes, **8** and **16**, in each series. Similarly, the constituent OEP rings in (*Z*)-bis(OEP)–M proved to be electronically more isolated as compared with those in the corresponding (*E*)-bis(OEP)–M, but reversely the transannular interaction between the face-to-face OEP rings in (*Z*)-bis(OEP)–M was suggested to give rise to the peculiarities in reactivity, spectral behavior, and electrochemical property, depending on the kind of the incorporated metals. In consequence, oligomerization of OEP rings with the vinylene-linkage makes their HOMO-LUMO gaps reduce regularly, while metalation with the heavier d^8 transition-metal ions makes their HOMO-LUMO gaps increase more intensively with impeding the π-electronic conjugation throughout the whole molecule.

Further studies on the electronic properties of various mixed metal complexes, bis(OEP)–(M1–M2) and tris(OEP)–(M1–M2–M3),[19] as well as on the structural properties of their oxidation products are now in progress.

Experimental

The melting points were determined on a hot-stage apparatus and are uncorrected. IR spectra were measured on a JASCO FT/IR 7300 spectrophotometer as KBr disks, unless otherwise stated; only significant absorptions are reported. Electronic absorption spectra were measured in $CHCl_3$ solution on a Shimadzu UV-2200A spectrophotometer (sh = shoulder). ^{1}H NMR spectra were measured in $CDCl_3$ solution on JEOL α-400 (400 MHz) spectrometers and were recorded in δ-values with TMS as an internal standard. FAB mass spectra were recorded with a JEOL AX-505 spectrometer using *m*-nitrobenzyl alcohol (NBA) as a matrix agent. Cyclic voltammetry was performed on a BAS CV-27 under the conditions shown in Table 4. Silica gel (Daiso gel 100IW or Merck 60) was used for column chromatography. $CHCl_3$ was distilled over calcium hydride and THF was distilled from sodium benzophenone ketyl under argon before use. The reactions were followed by TLC aluminum sheets precoated with Merck silica gel F_{254} or with Merck aluminum oxide GF_{254}. Organic extracts were dried over anhydrous sodium sulfate or magnesium sulfate prior to removal of the solvents. The compounds **1—4** and **5** and **9** were prepared according to the reported procedures, as mentioned in the text.

Dinickel(II) (*E*)- and (*Z*)-Complexes of 5,5′-Vinylenebis(2,3,7,8,12,13,17,18-octaethylporphyrin) (6 and 10): The mixture of (*E*)-bis(OEP)–H_2 **5**[2] (20 mg, 0.018 mmol) and $Ni(OAc)_2 \cdot H_2O$ (89.6 mg, 0.36 mmol) in DMF (30 cm^3) was stirred at 110 °C for 5 h.[8] After being poured into water, the reaction mixture was extracted with $CHCl_3$, washed with brine thoroughly, and then dried. The residue obtained after removal of solvent was chromatographed on silica gel (3.8×5 cm) with $CHCl_3$ to afford the (*E*)-isomer **6** (19.4 mg, 88%) as the first fractions. The later fractions afforded the (*Z*)-isomer **10** (1.5 mg, 6.8%).

6:[2] Black purple microcrystals (hexane–$CHCl_3$); ^{1}H NMR δ = 9.50 (2H, s, *meso*-H), 9.48 (4H, s, *meso*-H), 7.66 (2H, s, –CH=CH–), 3.88 (16H, q, *J* = 7.5 Hz, –CH_2–), 3.76 (8H, q, *J* = 7.5 Hz, –CH_2–), 3.40 (8H, br s, –CH_2–), 1.85—1.70 (36H, m, CH_3), 1.02 (12H, t, *J* = 7.5 Hz, CH_3).

10:[8] Black purple microcrystals (hexane–$CHCl_3$); ^1H NMR $\delta = 9.29$ (2H, s, –CH=CH–), 9.05 (2H, s, *meso*-H), 8.06 (4H, s, *meso*-H), 4.02 (4H, dq, $J = 7.5$ and 15 Hz, –CH_2–), 3.86 (4H, dq, $J = 7.5$ and 15 Hz, –CH_2–), 3.76 (4H, dq, $J = 7.5$ and 15 Hz, –CH_2–), 3.59 (4H, dq, $J = 7.5$ and 15 Hz, –CH_2–), 3.49 (4H, dq, $J = 7.5$ and 15 Hz, –CH_2–), 2.89 (4H, dq, $J = 7.5$ and 15 Hz, –CH_2–), 2.66 (4H, dq, $J = 7.5$ and 15 Hz, –CH_2–), 2.59 (4H, dq, $J = 7.5$ and 15 Hz, –CH_2–), 1.81 (12H, t, $J = 7.5$ Hz, CH_3), 1.50 (12H, t, $J = 7.5$ Hz, CH_3), 1.44 (12H, t, $J = 7.5$ Hz, CH_3), 0.69 (12H, t, $J = 7.5$ Hz, CH_3).

Dipalladium(II) (*E*)- and (*Z*)-Complexes of 5,5′-Vinylenebis-(2,3,7,8,12,13,17,18-octaethylporphyrin) (7 and 11): The mixture of **5**[2] (20 mg, 0.018 mmol) and $Pd(OAc)_2$ (80.8 mg, 0.36 mmol) in $CHCl_3$–MeOH (4 : 1 v/v, 30 cm^3) was refluxed with stirring gently for 3 h. After being poured into water, the reaction mixture was extracted with $CHCl_3$, washed with brine, and then dried. The residue obtained after removal of solvent was chromatographed on silica gel (3.2×5 cm) with $CHCl_3$ to afford the (*E*)-isomer **7** (21.5 mg, 90%) as the first fractions. The later fractions afforded the (*Z*)-isomer **11** (1.2 mg, 5.0%).

7: Reddish purple microcrystals (hexane–$CHCl_3$); mp > 300 °C; Mass (FAB) *m/z* 1303 (M^++1); IR (KBr) 2955, 2930, and 2865 cm^{-1} (CH); ^1H NMR $\delta = 10.10$ (4H, s, *meso*-H), 10.02 (2H, s, *meso*-H), 8.15 (2H, s, –CH=CH–), 4.16 (16H, q, $J = 7.5$ Hz, –CH_2–), 3.72 (8H, q, $J = 7.5$ Hz, –CH_2–), 3.55 (8H, br s, –CH_2–), 2.1—1.8 (12H, m, CH_3), 1.3—1.1 (24H, m, CH_3), 0.92 (12H, t, $J = 7.5$ Hz, CH_3). Found: C, 68.01; H, 7.00; N, 8.87%. Calcd for $C_{74}H_{88}N_8Pd_2$: C, 68.24; H, 6.81; N, 8.61%.

11: Reddish purple microcrystals (hexane–$CHCl_3$); mp > 300 °C; Mass (FAB) *m/z* 1303 (M^++1); IR (KBr) 2960, 2935, and 2870 cm^{-1} (CH); ^1H NMR $\delta = 9.55$ (2H, s, –CH=CH–), 9.26 (2H, s, *meso*-H), 8.15 (4H, s, *meso*-H), 4.42 (4H, dq, $J = 7.5$ and 15 Hz, –CH_2–), 4.22 (4H, dq, $J = 7.5$ and 15 Hz, –CH_2–), 3.88 (4H, dq, $J = 7.5$ and 15 Hz, –CH_2–), 3.64 (4H, dq, $J = 7.5$ and 15 Hz, –CH_2–), 3.48 (8H, m, –CH_2–), 3.22 (4H, dq, $J = 7.5$ and 15 Hz, –CH_2–), 3.11 (4H, dq, $J = 7.5$ and 15 Hz, –CH_2–), 1.78 (12H, t, $J = 7.5$ Hz, CH_3), 1.58—1.52 (24H, m, CH_3), 1.22 (12H, t, $J = 7.5$ Hz, CH_3). Found: C, 67.98; H, 6.93; N, 8.55%. Calcd for $C_{74}H_{88}N_8Pd_2$: C, 68.24; H, 6.81; N, 8.61%.

Diplatinum(II) (*E*)- and (*Z*)-Complexes of 5,5′-Vinylenebis(2,3,7,8,12,13,17,18-octaethylporphyrin) (8 and 12): The mixture of **5**[2] (20 mg, 0.018 mmol) and $Pt(acac)_2$ (141 mg, 0.36 mmol) in PhOH (30 cm^3) was stirred at 155—160 °C for 5 h. After being poured into water, the reaction mixture was extracted with $CHCl_3$, washed with sat. sodium hydrogencarbonate aq thoroughly, and with brine, and then dried. The residue obtained after removal of solvent was chromatographed on silica gel (3.8×6 cm) with $CHCl_3$–ethyl acetate to afford the (*E*)-isomer **8** (20.9 mg, 77%) as the first fractions. The later fractions afforded the (*Z*)-isomer **12** (3.0 mg, 11%).

8: Reddish purple microcrystals (hexane–$CHCl_3$); mp > 300 °C; Mass (FAB) *m/z* 1480 (M^++1); IR (KBr) 2960, 2930, and 2875 cm^{-1} (CH); ^1H NMR $\delta = 10.02$ (4H, s, *meso*-H), 9.96 (2H, s, *meso*-H), 8.17 (2H, s, –CH=CH–), 4.07 (16H, q, $J = 7.5$ Hz, –CH_2–), 3.7—3.6 (16H, m, –CH_2–), 2.0—1.9 (12H, m, CH_3), 1.3—1.2 (24H, m, CH_3), 0.96 (12H, t, $J = 7.5$ Hz, CH_3). Found: C, 59.85; H, 6.22; N, 7.46%. Calcd for $C_{74}H_{88}N_8Pt_2$: C, 60.06; H, 5.99; N, 7.57%.

12: Reddish purple microcrystals (hexane–$CHCl_3$); mp > 300 °C; Mass (FAB) *m/z* 1480 (M^++1); IR (KBr) 2960, 2930, and 2870 cm^{-1} (CH); ^1H NMR $\delta = 9.39$ (2H, s, –CH=CH–), 9.21 (2H, s, *meso*-H), 8.12 (4H, s, *meso*-H), 4.43 (4H, dq, $J = 7.5$ and 15 Hz, –CH_2–), 4.20 (4H, dq, $J = 7.5$ and 15 Hz, –CH_2–), 3.90 (4H, dq, $J = 7.5$ and 15 Hz, –CH_2–), 3.66 (4H, dq, $J = 7.5$ and 15 Hz, –CH_2–), 3.49 (8H, m, –CH_2–), 3.19 (4H, dq, $J = 7.5$ and 15 Hz, –CH_2–), 3.08 (4H, dq, $J = 7.5$ and 15 Hz, –CH_2–), 1.75 (12H, t, $J = 7.5$ Hz, CH_3), 1.6—1.5 (24H, m, CH_3), 1.20 (12H, t, $J = 7.5$ Hz, CH_3). Found: C, 59.73; H, 6.25; N, 7.33%.Calcd for $C_{74}H_{88}N_8Pt_2$: C, 60.06; H, 5.99; N, 7.57%.

Trinickel(II) Complex of (*E,E*)-5,15-Bis[2-(2,3,7,8,12,13,17,18-octaethyl-5-porphyrinyl)vinyl]-2,3,7,8,12,13,17,18-octaethylporphyrin (14): **14** was prepared from (*E,E*)-tris(OEP)–H_2 **13** by way of the previously reported procedure.[5] Black microcrystals (hexane–$CHCl_3$); ^1H NMR $\delta = 10.08$ (4H, br s, *meso*-H), 10.04 (2H, s, *meso*-H), 9.99 (2H, s, *meso*-H,), 8.16 (2H, d, $J = 15$ Hz, –CH=CH–), 8.03 (2H, br d, $J = 15$ Hz, –CH=CH–), 4.2—3.2 (48H, m, CH_2), 2.1—1.9 (48H, m, CH_3), 1.3—1.1 (24H, m, CH_3).

Tripalladium(II) Complex of (*E,E*)-5,15-Bis[2-(2,3,7,8,12,13,17,18-octaethyl-5-porphyrinyl)vinyl]-2,3,7,8,12,13,17,18-octaethylporphyrin (15): The mixture of **13**[5] (20 mg, 0.012 mmol) and $Pd(OAc)_2$ (80.8 mg, 0.36 mmol) in a mixture of $CHCl_3$–MeOH (4 : 1 v/v, 30 cm^3) was refluxed for 1.5 h. After being poured into water, the reaction mixture was extracted with $CHCl_3$, washed with brine, and then dried. The residue obtained after removal of solvent was chromatographed on silica gel (3.4×5 cm) with $CHCl_3$–ethyl acetate to afford **15**[11] (23 mg, 96%) as the main and sole product. Sparkling reddish purple microcrystals (hexane–$CHCl_3$); mp > 300 °C; Mass (FAB) *m/z* 1966 (M^++1); IR (KBr) 2960, 2930, and 2860 cm^{-1} (CH); ^1H NMR $\delta = 10.08$ (4H, br s, *meso*-H), 10.04 (2H, s, *meso*-H), 9.99 (2H, s, *meso*-H), 8.16 (2H, d, $J = 15$ Hz, –CH=CH–), 8.03 (2H, br d, $J = 15$ Hz, –CH=CH–), 4.2—3.2 (48H, m, CH_2), 2.1—1.9 (48H, m, CH_3), 1.3—1.1 (24H, m, CH_3). Found: C, 68.72; H, 6.78; N, 8.27%. Calcd for $C_{112}H_{132}N_{12}Pd_3$: C, 68.42; H, 6.77; N, 8.56%.

Triplatinum(II) Complex of (*E,E*)-5,15-Bis[2-(2,3,7,8,12,13,17,18-octaethyl-5-porphyrinyl)vinyl]-2,3,7,8,12,13,17,18-octaethylporphyrin (16): The mixture of **13**[5] (20.6 mg, 0.0125 mmol) and $PtCl_2$ (60.5 mg, 0.246 mmol) in AcOH (15 cm^3) was refluxed for 6 h. After being poured into water and neutralized with sat. sodium bicarbonate aq, the reaction mixture was extracted with $CHCl_3$, washed with brine, and then dried. The residue obtained after removal of solvent was chromatographed on silica gel (3.2×12 cm) with $CHCl_3$ to afford **16** (7.9 mg, 28.3%). Sparkling reddish purple microcrystals (hexane–$CHCl_3$); mp > 300 °C; Mass (FAB) *m/z* 2232 (M^++1); IR (KBr) 2960, 2925, and 2850 cm^{-1} (CH); ^1H NMR $\delta = 10.01$ (4H, br s, *meso*-H), 9.97 (2H, s, *meso*-H), 9.93 (2H, s, *meso*-H), 8.19 (2H, d, $J = 15$ Hz, –CH=CH–), 8.03 (2H, br d, $J = 15$ Hz, –CH=CH–), 4.2—3.3 (48H, m, CH_2), 2.1—0.7 (72H, m, CH_3). Found: C, 60.05; H, 6.22; N, 7.30%. Calcd for $C_{112}H_{132}N_{12}Pt_3$: C, 60.30; H, 5.92; N, 7.54%.

H. H. expresses his thanks to Dr. Keisuke Umakoshi at Hokkaido University for his generous supply of the platination reagent (*c*-[$PtCl_2(NH_3)_2$]) and to Prof. Koji Yamamoto at Osaka Prefecture University for useful and helpful discussions, and special acknowledgment to The Ministry of Education, Science, Sports and Culture, for the financial support by a Grant-in-Aid for Scientific Research No. 08454199.

References

1 M. R. Wasielewski, *Chem. Rev.*, **92**, 435 (1992); J. L. Sessler, V. L. Capuano, and A. Harriman, *J. Am. Chem. Soc.*, **115**, 4618

(1993); A. Osuka, N. Tanabe, S. Kawabata, I. Yamazaki, and Y. Nishimura, *J. Org. Chem.*, **60**, 7177 (1995); P. J. Angiolillo, V. S. -V. Lin, J. M. Vanderkooi, and M. J. Therien, *J. Am. Chem. Soc.*, **117**, 12514 (1995); A. Giraudeau, L. Ruhlmann, L. E. Kahef, and M. Gross, *J. Am. Chem. Soc.*, **118**, 2969 (1996); J. P. Strachan, S. Gentemann, J. Seth, W. A. Kalsbeck, J. S. Lindsey, D. Holten, and D. F. Bocian, *J. Am. Chem. Soc.*, **119**, 11191 (1997); O. Mongin, C. Papamicael, N. Hoyler, and A. Gossauer, *J. Org. Chem.*, **63**, 5568 (1998); R. W. Wagner, J. Seth, S. I. Yang, D. Kim, D. F. Bocian, D. Holton, and J. S. Linsey, *J. Org. Chem.*, **63**, 5042 (1998); H. Levanon, T. Galili, A. Regev, G. P. Wiederrecht, W. A. Svec, and M. R. Wasielewski, *J. Am. Chem. Soc.*, **120**, 6366 (1998), and many other references cited therein.

2 G. V. Ponomarev and A. M. Shul'ga, *Khim. Geterotski. Soed.*, **1986**, 278.

3 a) J. Deisenhofer, O. Epp, K. Miki, R. Huber, and H. Michel, *J. Mol. Biol.*, **180**, 385 (1984). b) M. O. Senge, M. G. H. Vicente, K. R. Gerzevske, T. P. Forsyth, and K. M. Smith, *Inorg. Chem.*, **33**, 5625 (1994), and references cited therein.

4 A. M. Shul'ga and G. V. Ponomarev, *Khim. Geterotski. Soed.*, **1988**, 339; G. V. Ponomarev, D. V. Yashunsky, and D. P. Arnold, *Recent Res. Devel. Pure Appl. Chem.*, **2**, 199 (1998).

5 H. Higuchi, K. Shimizu, J. Ojima, K. Sugiura, and Y. Sakata, *Tetrahedron Lett.*, **36**, 5359 (1995).

6 H. Higuchi, K. Shimizu, M. Takeuchi, J. Ojima, K. Sugiura, and Y. Sakata, *Bull. Chem. Soc. Jpn.*, **70**, 1923 (1997), and Ref. 19.

7 a) J. W. Buchler, in "The Porphyrins," ed by D. Dolphin, Academic Press, New York (1978), Vol. I, pp. 389—483. b) M. Gouterman, in "The Porphyrins," ed by D. Dolphin, Academic Press, New York (1978), Vol. III, pp. 1—165.

8 a) G. V. Ponomarev, V. V. Borovkov, K. Sugiura, Y. Sakata, and A. M. Shul'ga, *Tetrahedron Lett.*, **34**, 2153 (1993). b) G. V. Ponomarev, V. V. Borokov, A. M. Shul'ga, and Y. Sakata, *J. Chem. Soc., Chem. Commun.*, **1994**, 1927.

9 a) J. W. Buchler and L. Puppe, *Liebigs Ann. Chem.*, **1970**, 142. b) J. W. Buchler and L. Puppe, *Liebigs Ann. Chem.*, **1974**, 1046.

10 Although no description of the reaction time for isomerization of **5** was given in the reported study,[8a] it took more than two weeks to reach the steady state equilibrated between **5** and **9** in our experiments. On the other hand, interconversion of the vinylene-linkage between (*E*)- and (*Z*)-configurations was also observed for the monometalated complexes, which are to be described as bis(OEP)–(M, H_2), under the same conditions more swiftly than for the free-base **5**, affording the corresponding equilibrium mixtures. The respective ratios of (*E*)- and (*Z*)-configurational isomers were found to depend on the kind of incorporated metals. The results as well as the mechanistic aspect will be reported in detail elsewhere.

11 Synthesis of the Pd complex **15** has been presented: M. Takeuchi, H. Hasegawa, H. Higuchi, and J. Ojima, "The 13th Symposium on Fundamental Organic Chemistry," Nagoya, Abstr., p. 222 (1996). Electronic spectral property of **15** has been preliminarily reported: H. Higuchi, M. Takeuchi, and J. Ojima, *Chem. Lett.*, **1996**, 593.

12 Also called "Payrone salt": M. Peyrone, *Justus Liebigs Ann. Chem.*, **51**, 1 (1844).

13 T. A. Stephenson, S. M. Morehouse, A. R. Powell, J. P. Haffer, and G. Wilkinson, *J. Chem. Soc.*, **1965**, 3632; M. A. A. F. de C. T. Carrondo and A. C. Skapski, *J. Chem. Soc., Chem. Commun.*, **1976**, 410.

14 T. R. Janson and J. J. Katz, in "The Porphyrins," ed by D. Dolphin, Academic Press, New York (1978), Vol. IV, pp. 1—59.

15 K. Maruyama, T. Nagata, and A. Osuka, *J. Phys. Org. Chem.*, **1988**, 63.

16 R. Takigawa, Y. Kai, G. V. Ponomarev, K. Sugiura, V. V. Borovkov, T. Kaneda, and Y. Sakata, *Chem. Lett.*, **1993**, 1071.

17 a) The free-bases, **5**, **9**, and **13**, exhibited the redox behaviors distinctly from the other metal complexes, where the respective voltammograms at the first scan shifted on continuation of scan toward the final voltammograms with reversible redox waves, depending on scan rates. b) For the electrochemical isomerization of **9** to **5**: D. P. Arnold, V. V. Borovkov, and G. V. Ponomarev, *Chem. Lett.*, **1996**, 485.

18 J. -H. Fuhrhop, K. M. Kadish, and D. G. Davis, *J. Am. Chem. Soc.*, **95**, 5140 (1973).

19 Some mixted metal complexes described as tris(OEP)–(M1–M2–M3) have been already synthesized as well. A part of physical properties of the tris(OEP)–(Ni–Pd–Pt) complex, of which three constituent OEP rings carry Ni(II), Pd(II), and Pt(II) ions in order of atomic number, has been preliminarily reported: M. Takeuchi, M. Shinbo, Y. Hasegawa, H. Higuchi, and J. Ojima, "The 74th National Meeting of Chemical Society of Japan," Kyoto, Abstr., No. 1 D3 10, p. 890 (1998). Experimental results for the structural properties of the oxidation products from not only the title complexes but also these mixed ones will be reported elsewhere.